

Note

## NIR chemical imaging to guide/support BMS-561389 tablet formulation development

L.R. Hilden<sup>a,\*</sup>, C.J. Pommier<sup>a</sup>, S.I.F. Badawy<sup>a</sup>, Emil M. Friedman<sup>b</sup>

<sup>a</sup> Bristol-Myers Squibb Co., P.O. Box 191, New Brunswick, NJ 08903-0191, USA

<sup>b</sup> 2304 Richmond Road, Beachwood, OH 44122, United States

Received 20 December 2006; received in revised form 19 November 2007; accepted 20 November 2007

Available online 24 November 2007

### Abstract

The objective of this study was to determine whether the particle size of extra-granular tartaric acid affects the uniformity of its distribution within BMS-561389 tablets. A near-infrared imaging technique was used to assess the distribution of tartaric acid near the surface of tablet tops and bottoms. Three batches of BMS-561389 tablets were manufactured using three lots of granular tartaric acid having different particle size distributions. Near-Infrared chemical images were acquired on the tops and bottoms of 15 tablets from each lot. Spectra were collected from 1350 to 1600 nm in 10 nm increments and 16 co-added scans at each wavelength. Data were analyzed using ISys™ 3.1 (Spectral Dimensions, Inc.) Chemical Imaging Software. Data analysis consisted of preprocessing, principal component analysis, and image analysis of the principal component scores image. It was feasible to map tartaric acid particles near the surface of BMS-561389 tablets using near infrared chemical imaging. The tartaric acid particle size statistics based on image analysis results correlated well with pre-compaction measurements using a laser-light scattering method. The image analysis results indicate that segregation of tartaric acid between tablet tops and bottoms was apparent in tablets lots containing both the largest and intermediate-size tartaric acid particles. For tablets made with the smallest tartaric acid particles, differences between tablet tops and bottoms in either the number of tartaric acid particles or the percent tablet surface area covered by tartaric acid were not statistically different at the 95% confidence level.

© 2007 Elsevier B.V. All rights reserved.

**Keywords:** Image analysis; Near-infrared reflectance spectroscopy; Particle size; Principal component analysis; Tablet excipients

### 1. Introduction

BMS-561389 (Razaxaban) is a novel, potent, selective and orally bioavailable direct Factor X<sub>a</sub> inhibitor. The free base form of BMS-561389 is a weak base with very low intrinsic solubility. It has pH dependent solubility with higher solubility at acidic pH values that decrease as the pH is increased. The hydrochloride salt was selected for development. Bioavailability of BMS-561389 was found to be dependent on the gastric pH whereby significant reduction in plasma AUC and C<sub>max</sub> was observed when BMS-561389 tablets were co-administered with H<sub>2</sub> receptor antagonists. The reduction in bioavailability was attributed to form conversion and precipitation of the poorly soluble free base during the initial dissolution of the salt. Incorporation of approximately 17% (w/w) tartaric acid enhanced dissolution behavior and bioavailability of BMS-561389 at the elevated gastric pH condition. Tartaric acid helps to decrease the micro-environmental pH and thus increase the solubility of BMS-561389 in the local environment of the dissolving dosage form. This increase in solubility leads to a lower degree of supersaturation in the micro-environment hence minimizing free base precipitation during dissolution of the hydrochloride salt. Once diluted into the bulk medium, the drug is capable of remaining in a supersaturated solution for an extended period of time, providing an opportunity for drug absorption to take place (Badawy et al., 2006). As a result, development of a BMS-561389 tablet dosage form containing tartaric acid was pursued.

While tartaric acid resulted in the bioavailability benefit described above, its incorporation in the tablet formulation created some processing difficulties. The addition of tartaric acid during the wet granulation manufacturing process was found to diminish the chemical stability of the tablets upon storage. As a result, a manufacturing process was designed in which tartaric

While tartaric acid resulted in the bioavailability benefit described above, its incorporation in the tablet formulation created some processing difficulties. The addition of tartaric acid during the wet granulation manufacturing process was found to diminish the chemical stability of the tablets upon storage. As a result, a manufacturing process was designed in which tartaric

\* Corresponding author. Current address: Eli Lilly and Company, Lilly Corporate Center, Indianapolis, IN 46285, United States. Tel.: +1 317 433 8272.

E-mail address: [Hilden.Lori\\_R@lilly.com](mailto:Hilden.Lori_R@lilly.com) (L.R. Hilden).

acid was incorporated in the formulation as an extra-granular component after drying and milling of the wet granulation. When a powder grade of tartaric acid was used in the formulation, sticking issues were encountered which were attributed to adhesion of tartaric acid to the compression tooling. A granular grade of tartaric acid was used instead as it was found to significantly reduce the filming and sticking during compression. However, the use of granular tartaric acid could potentially lead to blend segregation during final blend transfer and/or tablet compression.

The objective of this study was to examine the effect of particle size of granular tartaric acid on the uniformity of its distribution within BMS-561389 tablets. Segregation of tartaric acid during die filling and/or the particle rearrangement stage of compression in the die may result in non-uniformity of its distribution within the tablet. Given that uniformity of tartaric acid distribution within the tablet may be critical for its optimal effect on bioavailability, a near-infrared imaging technique was used to assess the distribution of tartaric acid within the intact tablets. Near-infrared images were acquired on tablet tops and bottoms, near the surfaces. Although near-infrared imaging is not a surface technique, it is unlikely that the entire depth of the tablet was sampled. Several literature reports describe the application of this technique for determining content uniformity, particle size and distribution of sample components (Clarke, 2004; Lewis et al., 2004; Lyon et al., 2002). Reviews written by Reich (2005) and Luypaert et al. (2007) describe recent developments in the pharmaceutical domain, describing applications ranging from raw materials identification to final product release.

## 2. Methods

### 2.1. Tablet preparation

Three batches of BMS-561389 tablets were manufactured using three lots of granular tartaric acid having different particle size distributions. The tablets were manufactured by a high shear wet granulation process and contained microcrystalline cellulose (MCC) as the filler, 15.0% (w/w) BMS-561389, 16.7% (w/w) tartaric acid, 3.0% (w/w) hydroxypropyl cellulose (HPC), 1.5% (w/w) croscarmellose sodium (CCS), 0.5% (w/w) colloidal silicon dioxide and 0.5% (w/w) magnesium stearate. Granulation was carried out in a Fielder PMA-65 high shear granulator at a theoretical batch size of 11.7 kg. Water was used as the granulating liquid. BMS-561389 was blended with MCC, HPC and 1/2 of the CCS in the high shear mixer for 3 min at 200 rpm and high chopper speed. Using a peristaltic pump, 4.0 kg of water was subsequently added to the blend in the granulator at a rate of 0.8 kg/min. During water addition, the impeller speed was maintained at 200 rpm while the chopper speed was maintained at high. Following the complete addition of water, the wet granulation was wet massed for 30 s while maintaining the impeller speed at 200 rpm and the chopper speed at the high setting. The wet granulation was dried in a hot air convection oven at 50 °C to a moisture content of not more than 3.5%. The granulation was then milled using a cone mill fitted with a

20-mesh screen (850  $\mu\text{m}$ , 0.033"). The milled granulation was blended with tartaric acid, the remaining CCS and the colloidal silicon dioxide for 15 min in a V-blender. In the final step, magnesium stearate was added to the V-blender and blended for 10 min. The blend was compressed into round tablets with a target tablet weight of 90 mg and a target hardness of 7 Strong Cobb Units (SCU)<sup>1</sup> using a six station Korsch press, PH106, fitted with shallow concave 1/4" tooling. The resulting tablets had an average diameter of 6.4 mm and an average thickness of 2.3 mm.

### 2.2. Particle size analysis for tartaric acid

Particle size analysis was performed using a Mastersizer 200 laser-light scattering instrument with a Scirocco 2000 dry sample dispersion unit and ceramic venturi disperser (Malvern Instruments, Worcestershire, UK). The vibration feed rate was set at 70% and the dispersive air pressure at 3.5 bar. No sample preparation was performed; approximately 1 g of dry powder was scooped into the dry powder accessory unit using a small metal spatula.

### 2.3. HPLC assay for tartaric acid

To prepare samples for HPLC analysis, each tablet was dispersed in 25 mL of 50% methanol in water. The contents were hand shaken for 1 min followed by sonication and machine shaking for 5 and 45 min, respectively. Finally, the solutions were filtered through a 0.45  $\mu\text{m}$  nylon filter.

HPLC analysis was performed using a 3- $\mu\text{m}$ , 150 mm  $\times$  4.6 mm i.d. Phenomenex Luna C18 Column and a 7 min isocratic elution method. The mobile phase was comprised of 97.5% (v/v) water, 2.4% (v/v) methanol and 0.1% (v/v) phosphoric acid. The sample injection volume was 20  $\mu\text{L}$  and the mobile phase flow rate was set at 0.75 mL/min. Analysis was performed at 254 nm. The concentration of tartaric acid in each tablet was determined based on a fit of the integrated peak area to a 5-point standard curve.

### 2.4. NIR image acquisition

Near-infrared chemical images were acquired using a Spectral Dimensions Matrix NIR imaging system. Spectra were collected from 1350 to 1600 nm in increments of 10 nm with 16 co-added scans at each wavelength range. The tablets were placed on a mirror during imaging for ease of background elimination during processing. Prior to collection of data from the tablets, a Spectralon 99% reflectance standard (Labsphere Inc., North Sutton, NH) background image cube and a camera dark current image cube were obtained using the same parameters as used for the tablets. Fifteen tablets from each batch were randomly selected for analysis.

<sup>1</sup> Strong Cobb Units (SCU) is a unit of force used to measure the hardness of tablets in the pharmaceutical industry, 1 SCU  $\approx$  7 N.

## 2.5. NIR image analysis

Data were analyzed using ISys<sup>TM</sup> 3.1 (Spectral Dimensions, Inc.) Chemical Imaging Software. Data analysis consisted of preprocessing and processing steps. The first of the preprocessing steps was subtraction of the camera dark cube ( $D$ ) from the background ( $B$ ) and sample ( $S$ ) image cubes; background correction to correct the spatial and spectral response of the system followed by conversion from reflectance ( $R$ ) to  $\log(1/R)$ , a unit similar to absorbance ( $A$ ):

$$A = \log\left(\frac{1}{R}\right), \quad \text{where } R = \frac{(S - D)}{(B - D)}$$

To minimize variance from the background, a spatial mask was applied that eliminated pixels that were outside the tablet area. As a result, these pixels were not included in the statistics and the spectra from these pixels were ignored in PCA. Pixels that were “hot” or “cold” – meaning that they had an abnormally high or low response – were removed by replacing their value by the mean center of a  $3 \times 3$  “neighborhood” of surrounding pixels. The remaining spectra in the data set were mean centered and normalized to unit variance.

Representative images of a tablet top from lot 52250-195 before and after preprocessing steps are shown in Fig. 1. The image on the left is the initial, unprocessed image. From this image it can be seen that the diameter of the tablet is approximately 152 pixels. Based on an average tablet diameter of 6.4 mm, the diameter of each pixel is approximately  $42 \mu\text{m}$ . The image in the center is the result following masking where all non-tablet pixels were set to “not-a-number” thereby reducing the number of data points. The image on the right is the resulting image following the removal of hot or cold pixels and normalization using ‘Mean center to and scale to unit variance by spectrum’. Normalization is a method used to correct for path length or thickness differences (Barnes et al., 1989). On the tablet tops, the number 468 has been embedded (embossed) on the tablet surface. Following normalization, the embossing is barely distinguishable from the remaining surface of the tablet. In addition, the hot and cold (bad) pixels have been removed and are no longer visible.

A principal components analysis was performed on the pre-processed images. Eight principal components were calculated.

The scores images for each of the principal components calculated for a single tablet are shown in Fig. 2. Principal component 1 (PC 1) accounted for 97.2% of the total variance in the image, and PC 2 accounted for 2.3% of the variance. PC 3 contributed only 0.2% to the total variance and the remaining PCs combined contributed less than 0.17%. PCs 1–3 show some correlation to the visual images of the tablets. Interestingly, in PCs 4–8, the outline of the embossing marking on the tablet can be observed, but the embossing does not appear in PCs 1–3, indicating that the applied normalization effectively removed any significant contribution of the embossing to the variance in the images.

Principal component 2 was selected for particle size analysis, as the PC 2 loading spectrum most emphasized the differences between the tartaric acid and excipient spectra (Figs. 3 and 4). Fig. 3 shows the normalized spectra of a single pixel populated by tartaric acid and a single pixel populated by excipient. Fig. 4 shows the PCA loading spectra for a single pixel overlaid with the raw spectrum of that pixel. The spectra of the single pixels in the tablet correlate well with the spectra obtained by the pure components, improving confidence in the analysis. The main difference between the NIR spectra of the tartaric acid and the excipients is in the slope of the spectra between 1400 and 1500 nm. Generally speaking, region selection in chemometric analysis is based around defined peaks related to the functional groups in the molecule. However, in this case there were not significant molecular bands observable in the NIR spectra, so the region of most difference was selected, which was in a baseline. Second derivative preprocessing, which is a common preprocessing step in NIR, would have completely eliminated the most significant difference observed between the spectra and made this analysis less sensitive.

Since the loading spectrum of principal component 2 was found to be most closely related to the difference between the tartaric acid spectrum and the excipient spectrum, it was utilized for the selection of particles with a contour delineation tool. The contour tool allows the user to select a threshold and create a binary image showing the pixels above and below that threshold. However, the Isys image analysis particle statistics results can be affected by the choice of contour or threshold level. Typically, a user would adjust the level until the spatial feature of interest is surrounded by the contour. In this case, this seemingly straightforward process was somewhat complicated for the anal-

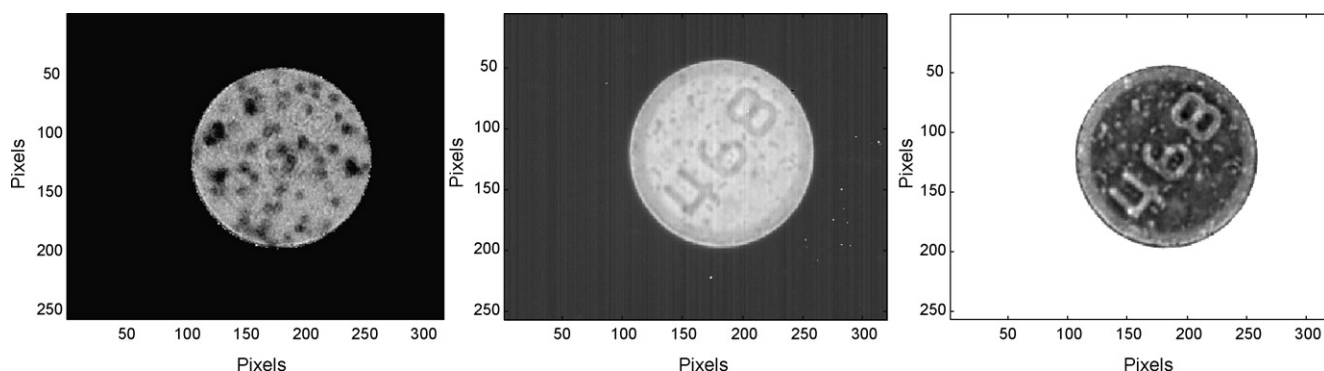


Fig. 1. Unprocessed image of top of tablet from lot 52250-195 (left), image following masking where all non-tablet pixels were set to “not-a-number” (middle) and image following normalization using ‘Mean center to and scale to unit variance by spectrum’ (right).

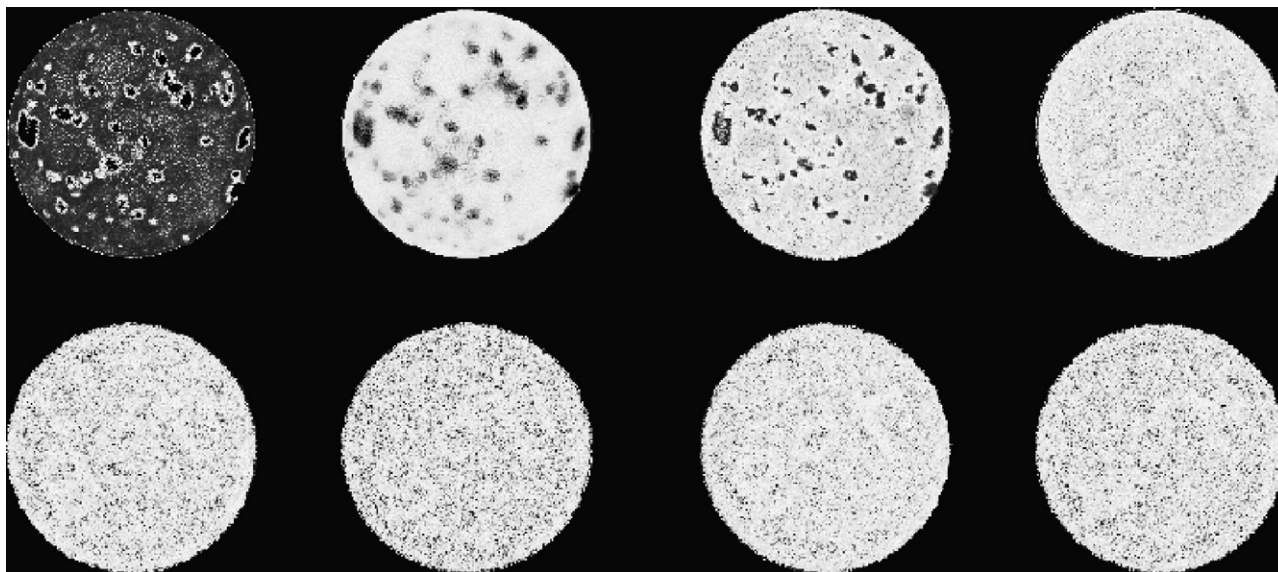


Fig. 2. PC score images of top of tablet from lot 195. Top row (L to R) PC 1 through PC 4. Bottom row (L to R) PC 5 through PC 8. PC 1 captured 97.19% of the variance in the image, PC 2 captured 2.34%, PC 3 captured 0.18%. PCs 4–8 each captured less than 0.08% of the variance of the image. Note that the embossing is visible in PCs 4–8, but is not obvious in PCs 1–3.

ysis of extra-granular tartaric acid. The difficulty arose when two or more particles lie in close proximity to each other making it difficult to distinguish them as separate, single particles. Optimally, a contour level should be selected that is capable of distinguishing between closely spaced particles and large single particles. The effect of contour level on particle statistics can be seen in Fig. 5. An image of the top of a tablet from lot 52250-195 is shown in the first row. The threshold was adjusted to a fine contour level ( $-0.71$ ) on the top left and adjusted to a coarse contour level ( $-0.14$ ) on the top right. In a similar fashion, an image of the tablet bottom is shown in the second row with a fine contour level ( $-0.71$ ) on the bottom left and a coarse contour level ( $-0.14$ ) on the bottom right. To give the reader perspective on these values, the practical range for setting the contour level ranged from approximately  $-0.9$  (extremely fine) to  $-0.1$  (extremely coarse). By setting the contour to a fine level, the user is able to differentiate closely spaced larger particles as separate particles. However, this results in fragments or chips broken off of larger particles during the compaction step being counted as individual particles. The opposite happens if a “coarse” contour level is used. Fragments of larger particles are not counted as individual particles, closely spaced particles are counted as a single particle, and the tablet surface between the closely spaced particles is included in the surface area of tartaric acid calculated.

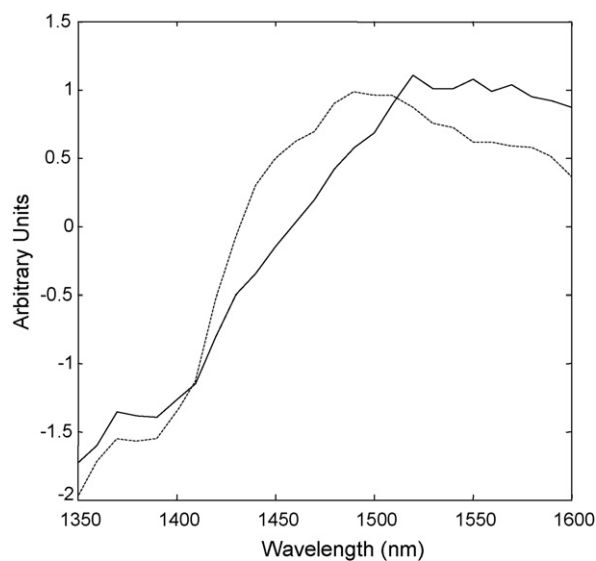


Fig. 3. Spectra of a single pixel populated by excipient (dashed line) or tartaric acid (solid line) after processing prior to PCA (background correction and normalization). The major difference in these spectra is the slope in the region from 1400 to 1500 nm. This region is best represented in PC 2.

Table 1  
Comparison of Isys™ particle statistics results based on PCA analysis of images of tablet tops and bottoms from lot 195 using a fine (left) or coarse (right) contour level

	Contour level	# Included particles	% Area covered	Mean equivalent diameter (pixels)	Mean equivalent diameter ( $\mu\text{m}$ )
Average top (St. Dev)	Fine	91.8 (19.9)	1.9 (0.4)	4.7 (0.7)	319.2 (29.4)
Average bottom (St. Dev)	Fine	86.1 (17.9)	1.6 (0.3)	4.5 (0.7)	315.0 (33.6)
Average top (St. Dev)	Coarse	27.3 (6.3)	5.9 (0.4)	13.9 (1.0)	583.8 (42.0)
Average bottom (St. Dev)	Coarse	29.3 (4.3)	5.9 (0.4)	15.3 (1.8)	642.6 (75.6)

For comparison, the D50 particle size statistic from Malvern measurements made on the pre-compacted material was 302.7  $\mu\text{m}$ .

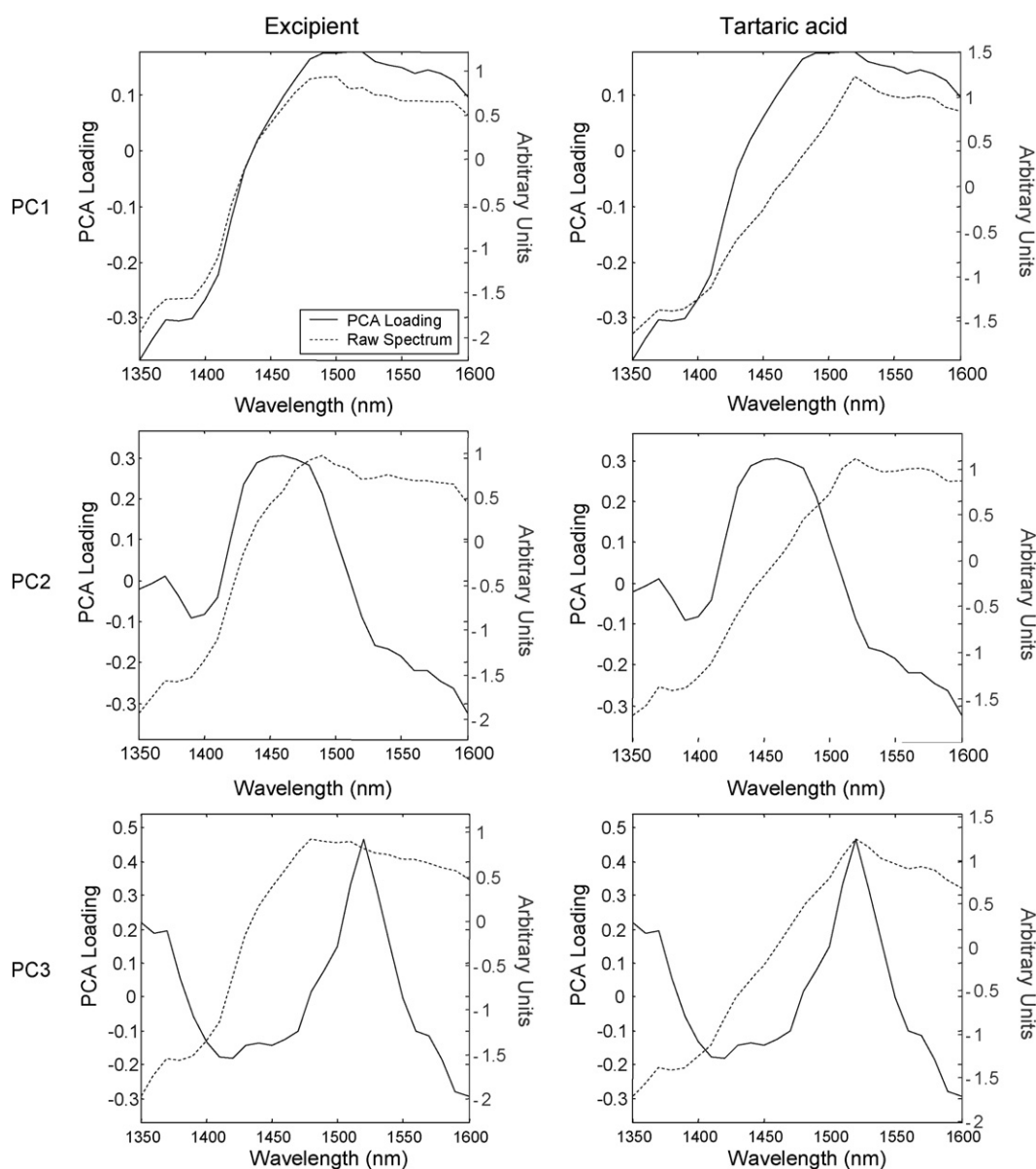


Fig. 4. PCA loading spectra for a single pixel overlaid with the raw spectrum of that pixel. Top left: raw spectrum (dotted) and PC 1 loading (solid) in a pixel populated by excipient. Middle left: raw spectrum (dotted) and PC 2 loading (solid) in a pixel populated by excipient. Bottom left: raw spectrum (dotted) and PC 3 loading (solid) in a pixel populated by excipient. Top right: raw spectrum (dotted) and PC 1 loading (solid) in a pixel populated by tartaric acid. Middle right: raw spectrum (dotted) and PC 2 loading (solid) in a pixel populated by tartaric acid. Bottom right: raw spectrum (dotted) and PC 3 loading (solid) in a pixel populated by tartaric acid.

This artificially raises the surface area and reduces the number of particles. For comparison, the particle statistics for all tablets from lot 52250-195, both top and bottom, were calculated using coarse and fine contour levels. The resulting particle statistics are listed in Table 1. As expected, the number of included particles was much higher and the percentage area covered was lower with the fine contour level as opposed to the coarse contour level.

A single contour level was selected and used for all images to minimize changes in observed particle size based on contributions from portions of partially buried particles. To select the appropriate contour level for the remaining analyses, the mean equivalent particle diameter resulting from particle statistics calculated at each contour level was compared with the median

pre-compaction particle size measured using the Malvern. The mean equivalent diameter represents the mean diameter of approximated circles, where each particle is approximated to a circle that occupies the same area as the particle. Particles with areas less than 6 pixels were omitted from this and subsequent analyses because 6 pixels is approximately 95  $\mu\text{m}$  (for spherical particles) and this is well below the lowest D10 value (149  $\mu\text{m}$ ) measured on the tartaric acid starting material. For tablet tops, the mean equivalent particle diameter was  $319 \pm 29 \mu\text{m}$  at the fine contour level and  $584 \pm 42 \mu\text{m}$  at the coarse level. For tablet bottoms, the mean equivalent particle diameter was  $315 \pm 34 \mu\text{m}$  at the fine contour level and  $642 \pm 76 \mu\text{m}$  using a coarse contour level. The Malvern D50

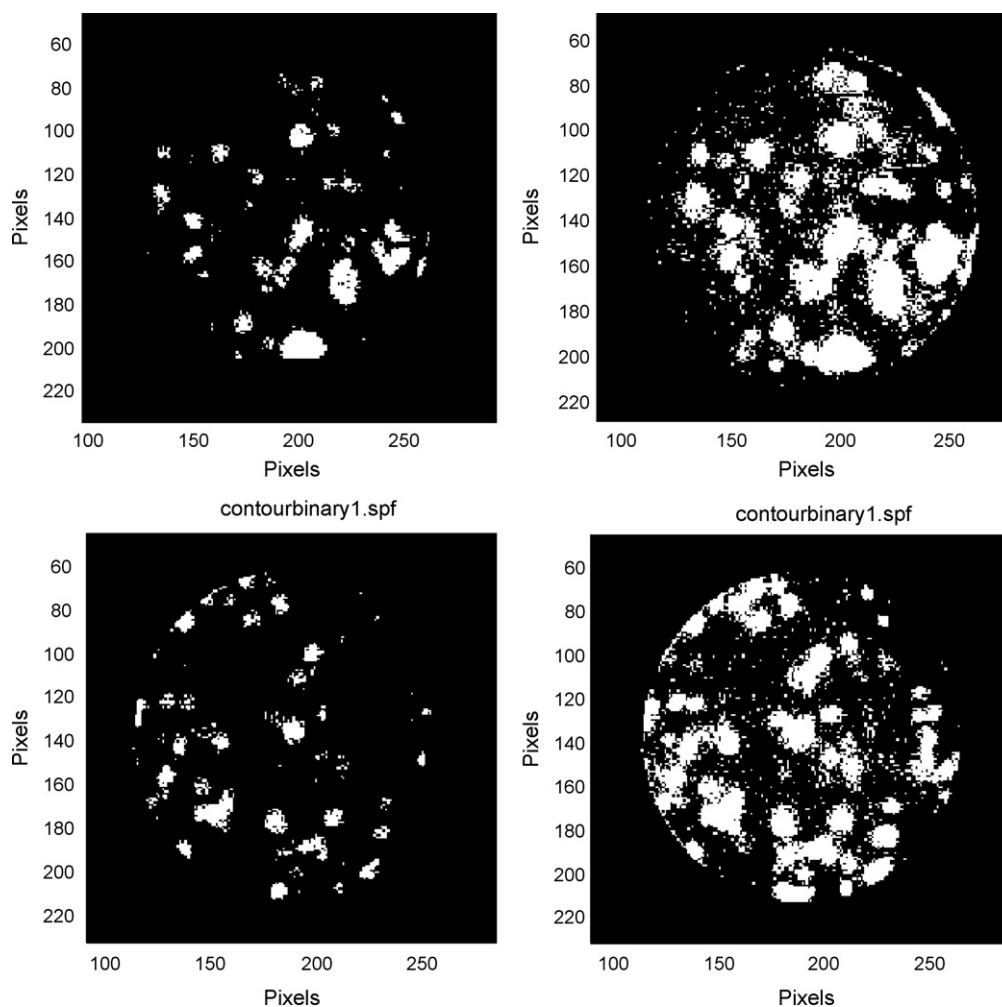


Fig. 5. Results of fine contour level (column 1) versus coarse contour level (column 2). All images are of tablet number 2 from lot 52250-195. The images from the tablet top are shown in the first row and the tablet bottom in the second row.

particle size for this lot was 302.7  $\mu\text{m}$ . Since the mean equivalent diameter from the particle statistics determined at the fine contour level of  $-0.71$  were most similar to the pre-compaction tartaric acid measurements made with the Malvern (based on an average pixel size of approximately 42  $\mu\text{m}$ ), the fine contour level was selected for all analyses.<sup>2</sup>

### 3. Results and discussion

The %R.S.D. of tartaric acid potency by HPLC ( $n = 5$ ) was 1.02, 0.75 and 2.15 for tablets that were imaged from lots 52250-186A, 52250-190 and 52250-195, respectively. These values indicate that tartaric acid was homogeneously distributed within the bulk granulation resulting in low variability in the tartaric acid content between tablets. However, such data does not permit conclusions to be drawn regarding the spatial distribution of tartaric acid within individual tablets.

<sup>2</sup> A fine vs. course contour level comparison was performed on only one of the three lots of tablets; thus, the apparent accuracy of the technique was not confirmed.

The D10, D50, D90 and D[4,3] particle size values for tartaric acid as measured by Malvern are listed in Table 2, according to tablet lot. Of the three lots of tablets, lot number 52250-186A contained the largest tartaric acid particles. The smallest tartaric acid particles were incorporated into tablet lot 52250-195. The width of the particle size distribution of tartaric acid in tablet lot 52250-190 was broader than in lots 52250-186A or 52250-195 and the measured particle size distribution was intermediate of the three lots used. The tartaric acid used in tablet lot 52250-190 was milled using a Fitz mill (hammer mill) to reduce the particle size of that particular lot to be within the range of interest for the study, the particle size range stated above is for the milled

Table 2

Malvern particle size analysis results for tartaric acid listed according to the tablet lot number in which the tartaric acid was incorporated

Tablet lot number	Particle size by Malvern ( $\mu\text{m}$ )			
	D10	D50	D90	D[4,3]
52250-186A	370.3	544.6	796.6	567.6
52250-190 (milled)	169.2	435.3	748.3	449.0
52250-195	149.1	302.7	569.9	331.2

material. The tartaric acid used in tablet lots 52250-186A and 52250-195 was not milled because the ‘as-is’ particle size fell within the range of interest.

The Isys™ particle size statistics values for the three tablet lots are listed in Table 3. The mean equivalent tartaric acid particle diameter, an average of the measurement from the 15 tops or bottoms from each tablet lot, is listed in units of pixels and microns in columns 1 and 2, respectively. The average number of (individual) particles having an area greater than 6 pixels (and therefore, included in the statistical analysis) is listed in column 3 and the average of the percent tablet surface area covered by tartaric acid is listed in the last column.

Lot 190 had more tartaric acid particles with area greater than 6 pixels per tablet top or bottom (Table 4) than either of the other two lots. The difference between the number of particles on the top and bottom of lot 186A is not statistically significant at 95% confidence.

The percent of the tablet surface area covered by tartaric acid, averaged over the top and bottom of each tablet, and the differences between the percent surface area covered by tartaric acid on tablet tops and bottoms are shown in Fig. 6. In terms of percent tablet surface area covered by tartaric acid, it is visually apparent that lot 186A had the greatest difference between tablet tops and bottoms, the most tartaric acid overall and the greatest variation. Lot 195 had the smallest difference between tablet tops and bottoms, the smallest percent area covered and the least variation. Lot 190 fell in between. The differences between lots, with respect to the percent of the tablet surface area covered by tartaric acid, were statistically significant ( $p \ll .05$ , Welch ANOVA for means; O’Brien, Brown-Forsyth, and Levene tests for variances). It is worth noting that lot 186A was produced using the coarsest tartaric acid and lot 195 the finest, but with only 3 lots of material, a discussion of causation based on statistics alone would be problematic. The top versus bottom difference was statistically significant for lots 186A and 190 (two-tailed  $t$ -test for paired data,  $p = .0008$  and  $p = .0005$ , respectively, each lot analyzed separately).

The difference in percent area covered by tartaric acid between top and bottom surfaces for lots 186A and 190 sug-

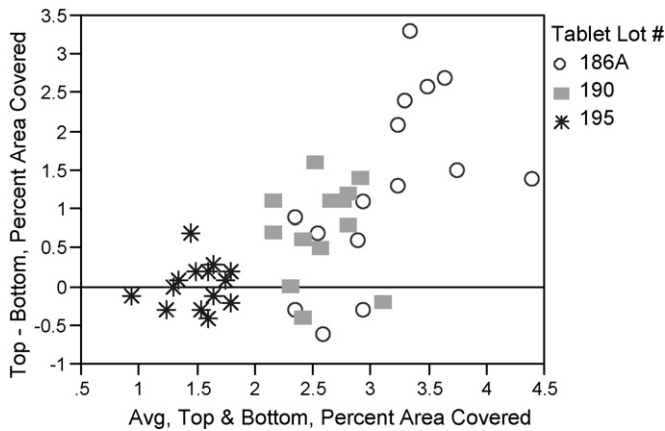


Fig. 6. Percent area covered by tartaric acid. The difference between tablet top and bottom versus the average of top and bottom are plotted. Plotting symbols identify the three lots.

Table 3  
Isys particle™ statistics results for extra-granular tartaric acid in tablets from lots 186A, 190 and 195

	Mean equivalent diameter (pixels)			Mean equivalent diameter (µm)			# Included particles			% Area covered		
	186A <sup>a</sup>	190 <sup>a</sup>	195 <sup>a</sup>	186A <sup>a</sup>	190 <sup>a</sup>	195 <sup>a</sup>	186A <sup>a</sup>	190 <sup>a</sup>	195 <sup>a</sup>	186A <sup>a</sup>	190 <sup>a</sup>	195 <sup>a</sup>
Avg. top (St. Dev)	13.0(2.2)	9.5 (1.3)	7.6 (0.7)	559.0(92.4)	399.0(54.6)	319.2 (29.4)	24.3(4.9)	34.3 (4.9)	28.4 (6.5)	3.9(1.0)	2.9 (0.4)	1.5 (0.3)
Avg. bottom (St. Dev)	9.9(1.9)	8.5 (1.2)	7.5 (0.8)	415.8(79.8)	357.0(50.4)	315.0 (33.6)	27.9(5.4)	32.5 (6.2)	27.5 (4.7)	2.5 (0.5)	2.2 (0.4)	1.5 (0.3)

A fine contour level (-0.71) was used for all analyses. The value listed is the average of the 15 tablet tops or bottoms sampled per lot. The standard deviation is listed in parentheses beside the average.  
<sup>a</sup> Tablet lot.

Table 4  
Number of tartaric acid particles per tablet top or bottom with area greater than 6 pixels

Lot	Difference top–bottom		Average of top and bottom	
	Difference	Standard deviation	Average	Standard deviation
186A	$-3.7 \pm 3.7$	6.7	$26.0 \pm 2.0$	3.7
190	$1.3 \pm 4.9$	8.4	$33.6 \pm 2.1$	3.7
195	$0.9 \pm 4.2$	7.5	$28.0 \pm 2.3$	4.2

Lot 190 was statistically different from lots 186A and 195 (Tukey-Kramer, HSD,  $p < 0.05$ ). All confidence intervals were 95%, each lot was analyzed separately.

gests some segregation of tartaric acid within the tablet. Tartaric acid is blended with milled granulation having a geometric mean diameter of 100–150  $\mu\text{m}$  as determined by mesh analysis. A large difference in particle size, therefore, exists between tartaric acid and the granules, which would promote segregation of the two components under certain conditions. The uniform tartaric acid distribution between tablets (as shown by the HPLC analysis) and the systematically higher percent covered for the top tablet surface suggests that segregation is taking place in the compression process and not in the preceding unit operations. Such segregation of tartaric acid can possibly occur in the initial particle rearrangement stage of compression where the smaller granules can percolate between the larger tartaric acid particles.

Since segregation is enhanced as the particle size difference between components is increased, it is expected that segregation of tartaric acid would be decreased by the reduction of its particle size. While it may be difficult to make firm conclusions with only three lots of tartaric acid tested, data presented above suggests that segregation is minimal for lot 195 and hence there was

no difference observed in the area covered between the top and bottom surfaces for this lot. It appears that segregation of tartaric acid within the tablet can be minimized when the tartaric acid D50 value approaches 300  $\mu\text{m}$ .

### Acknowledgements

The authors would like to acknowledge contributions from the following individuals: Jon Hilden—particle size analysis; David Gray—tablet preparation; Scott Huffman and John Randall—spectroscopic measurements.

### References

- Badawy, S.I.F., Gray, D.B., Zhao, F., Sun, D., Schuster, A.E., Hussain, M.A., 2006. Formulation of solid dosage forms to overcome gastric pH interaction of the factor  $X_a$  inhibitor, BMS-561389. *Pharm. Res.* 23, 989–996.
- Barnes, R.J., Dhanoa, M.S., Lister, S.J., 1989. Standard normal variate transformation and de-trending of near-infrared diffuse reflectance spectra. *Appl. Spectrosc.* 43, 772–777.
- Clarke, F., 2004. Extracting process-related information from pharmaceutical dosage forms using near infrared microscopy. *Vib. Spec.* 34, 25–35.
- Lewis, E.N., Schoppelrei, J., Lee, E., 2004. Near-infrared chemical imaging and the PAT initiative. *Spectroscopy* 19, 26–36.
- Luypaert, J., Massart, D.L., Vander Heyden, Y., 2007. Near-infrared spectroscopy applications in pharmaceutical analysis. *Talanta* 72, 865–883.
- Lyon, R.C., Lester, D.S., Lewis, E.N., Lee, E., Yu, L.X., Jefferson, E.H., Hussain, A.S., 2002. Near-infrared spectral imaging for quality assurance of pharmaceutical products: analysis of tablets to assess powder blend homogeneity. *AAPS Pharm. Sci. Tech.* 3, 1–15.
- Reich, G., 2005. Near-infrared spectroscopy and imaging: basic principles and pharmaceutical applications. *Adv. Drug Del. Rev.* 57, 1109–1143.